ScaleDoc: Scaling LLM-based Predicates over Large Document Collections

Hengrui Zhang*
Tsinghua University
zhanghen22@mails.tsinghua.edu.cn

Yulong Hui*
Tsinghua University
huiyl22@mails.tsinghua.edu.cn

Yihao Liu
Tsinghua University
liuyihao24@mails.tsinghua.edu.cn

Huanchen Zhang
Tsinghua University
huanchen@tsinghua.edu.cn

ABSTRACT

Predicates are foundational components in data analysis systems. However, modern workloads increasingly involve unstructured documents, which demands semantic understanding, beyond traditional value-based predicates. Given enormous documents and ad-hoc queries, while Large Language Models (LLMs) demonstrate powerful zero-shot capabilities, their high inference cost leads to unacceptable overhead. Therefore, we introduce ScaleDoc, a novel system that addresses this by decoupling predicate execution into an offline representation phase and an optimized online filtering phase. In the offline phase, ScaleDoc leverages a LLM to generate semantic representations for each document. Online, for each query, it trains a lightweight proxy model on these representations to filter the majority of documents, forwarding only the ambiguous cases to the LLM for final decision. Furthermore, ScaleDoc proposes two core innovations to achieve significant efficiency: (1) a contrastive-learning-based framework that trains the proxy model to generate reliable predicating decision scores; (2) an adaptive cascade mechanism that determines the effective filtering policy while meeting specific accuracy targets. Our evaluations across three datasets demonstrate that ScaleDoc achieves over a 2× end-to-end speedup and reduces expensive LLM invocations by up to 85%, making large-scale semantic analysis practical and efficient.

PVLDB Reference Format:
Hengrui Zhang*, Yulong Hui*, Yihao Liu, and Huanchen Zhang. ScaleDoc: Scaling LLM-based Predicates over Large Document Collections. PVLDB, 1(1): XXX-XXX, 2020.
doi:XX.XX/XXX.XX

PVLDB Artifact Availability:
The source code, data, and/or other artifacts have been made available at https://github.com/Seurgul/ScaleDoc.

1 INTRODUCTION

Predicates are essential for selecting relevant data in relational databases, search engines, and big-data systems. Traditionally, these systems have excelled at value-based predicates (e.g., CITY = 'Boston'). However, modern analytical tasks increasingly require querying enormous corpora of unstructured documents based on their semantic meaning [13]. For example, medical researchers might look for publications that "developed novel psychotropic medications," or enterprises may need to analyze reports where customers are "expressing dissatisfaction with service quality." Such queries require a deep contextual understanding that goes beyond simple keyword matching.

Handling ad-hoc semantic queries in large-scale analytics presents a significant challenge. Custom machine learning (ML) models are not scalable for this purpose because of the extensive engineering and data labeling effort required for each new task. While the advent of Large Language Models (LLMs) offers a solution with their remarkable zero-shot reasoning capabilities, their high computational cost creates a major barrier. The expense of running LLM inference across millions of documents for every query makes this approach impractical for widespread adoption [2].

Real-world semantic judgments are often ambiguous, making perfect accuracy costly and impractical. Consequently, many systems prioritize scalable efficiency by aiming for a specific accuracy target [15, 27, 35, 39]. To achieve this trade-off, some systems, such as NoScope [15] and PPs [27], use lightweight proxy models to filter easier cases. However, these methods are task-specific and lack zero-shot flexibility. More recent LLM-centric solutions, such as FrugalGPT [4] and Lotus [31], use smaller LLMs (e.g., GPT-3.5 or LLaMA-8B) as filtering proxies. While more flexible, these smaller LLMs remain too computationally expensive for truly large-scale applications involving millions of documents.

A critical inefficiency in current LLM-based approaches is the repetitive re-processing of entire documents for every ad-hoc query, incurring substantial and redundant computational costs. A key insight is to shift these expensive, document-centric LLM computations to a one-time offline phase to reduce the burden during online processing. We, therefore, propose ScaleDoc, a system designed for efficient LLM-based predicate execution over enormous document corpora. ScaleDoc decouples the execution into two phases. The one-time *offline representation* phase creates a rich semantic representation of each document using an LLM. Then, when an ad-hoc query arrives, the *online processing* phase trains a lightweight, query-specific proxy model that uses these representations to rapidly filter the document set. The model identifies and forwards only the most ambiguous documents to the powerful but expensive LLM, achieving significant efficiency gains while maintaining high accuracy.

* The authors contributed equally to this work.

Proceedings of the VLDB Endowment, Vol. 1, No. 1 ISSN 2150-8097.
doi:XX.XX/XXX.XX

While this architecture is promising, its effectiveness depends on overcoming two key challenges. First, the lightweight proxy model must be trained to provide reliable decisions. Since the proxy lacks the oracle LLM's deep semantic understanding, a basic training method can yield ambiguous decision scores that fail to separate positive and negative cases. Such ambiguity would render the proxy ineffective because most documents would be forwarded to the expensive oracle. To address this, we developed a framework based on *contrastive learning* that trains the proxy to capture fine-grained semantics and produce well-behaved predicating decision scores.

The second challenge is that the system must determine an effective filtering threshold for each ad-hoc query. Because the relationship between accuracy and decision scores is unknown for a new query, it is difficult to establish a threshold that meets a user's accuracy target while minimizing cost. We tackled this with an *adaptive cascade mechanism* that performs online calibration to shape query-specific score distributions, and then uses an optimized algorithm to determine the ideal thresholds.

We evaluated ScaleDoc across three diverse datasets, where it significantly outperforms existing baselines. On average, ScaleDoc achieves over a 2× end-to-end performance speedup and reduces costly LLM invocations by up to 85%.

Our paper makes the following contributions:

- We propose ScaleDoc, a novel system that decouples execution into a one-time offline representation phase and an optimized online query phase.
- We introduce a contrastive learning strategy to train a lightweight, query-aware proxy model that provides reliable scores to enable effective data filtering.
- We design an adaptive online calibration mechanism with an optimized threshold-selection algorithm to guarantee user-specified accuracy while minimizing calls to the expensive oracle LLM.

2 SYSTEM OVERVIEW

ScaleDoc provides an efficient solution for executing semantic predicates over large-scale documents. This section defines the target workloads, introduces the system's architecture, and outlines the core challenges need to overcome.

2.1 Workload Specification

ScaleDoc is designed to process boolean semantic predicates. We define the workload with a tuple, containing a document collection, a natural language query, and a user-specified accuracy target. Formally, a workload can be expressed in an SQL-like syntax. For instance, a query to find all medical papers in PubMed that develop a new drug would be:

```
SELECT * FROM PubMed
WHERE "The paper introduces a new drug"
WITH accuracy_target = 0.90
```

For each such workload, ScaleDoc executes the system pipeline , assigning each document as positive or negative while meeting the specified accuracy target.

2.2 System Architecture

ScaleDoc adopts an offline-online architecture, enabling efficient execution through the decoupling of query processing stages. An overview of the ScaleDoc pipeline is illustrated in Figure 1.

The offline stage is a one-time, compute-intensive process. For each document, we use a small-scale LLM (e.g., with 7B parameters) to generate a semantic embedding, which is then stored for online use. This approach offers two main benefits. First, it leverages the expressive power of the LLM to produce semantically rich document representations. This provides a high-quality foundation, allowing lightweight processing in subsequent online stages. Second, it front-loads the necessary yet expensive computations of LLM. By pre-computing and storing these embeddings, ScaleDoc can efficiently reuse them across countless ad-hoc queries, eliminating the need to repeatedly run the LLM.

The online stage employs a proxy-cascade architecture to handle ad-hoc queries efficiently. Upon receiving a new query, ScaleDoc will train a query-specific, lightweight proxy model. This model then rapidly evaluates the documents, assigning each a decision score, indicating the likelihood of the positive predicate. To train this model, we need first sample a small fraction (e.g., 5%) of the documents, and obtain ground-truth predicating labels by calling a powerful oracle LLM (e.g., GPT-4o [30]). After the proxy model, a subsequent cascade filter uses the proxy decision scores to decide the high-confidence and low-confidence documents. The proxy's judgment is adopted for the high-confidence set, while the low-confidence set is forwarded to the oracle LLM for a final judgment. This hierarchical approach strategically minimizes oracle invocations, ensuring scalable and cost-effective query execution.

2.3 Core Challenges

While this offline-online and proxy-oracle architecture is promising, its effectiveness hinges on overcoming two critical orchestration challenges:

Reliable Proxy Model. The efficiency of the cascade filter depends on the quality of the decision scores produced by the lightweight proxy model. A naive model might fail to capture the fine-grained semantics between the query and documents, leading to unreliable proxy predictions. Furthermore, a poorly trained model may generate ambiguous scores that do not clearly distinguish positive and negative documents. Such an ambiguity would force a large fraction of instances to be categorized as "uncertain", leading to excessive invocations of the expensive oracle LLM and diminishing the system's performance benefits. Therefore, the first challenge is to develop a well-behaved proxy model, capable of generating decisive and accurate scores, enabling maximum data reduction.

Ad-Hoc Cascade. Given the proxy model's scores, the cascade filter must determine the decision thresholds to separate documents into high-confidence (to be filtered) and low-confidence (to be verified by the oracle) sets. The goal is to meet the user-specified accuracy target while minimizing the number of oracle calls. However, in an ad-hoc setting, neither the query-specific data distribution nor the ground-truth labels are known beforehand. This lack of prior knowledge makes it non-trivial to select effective thresholds

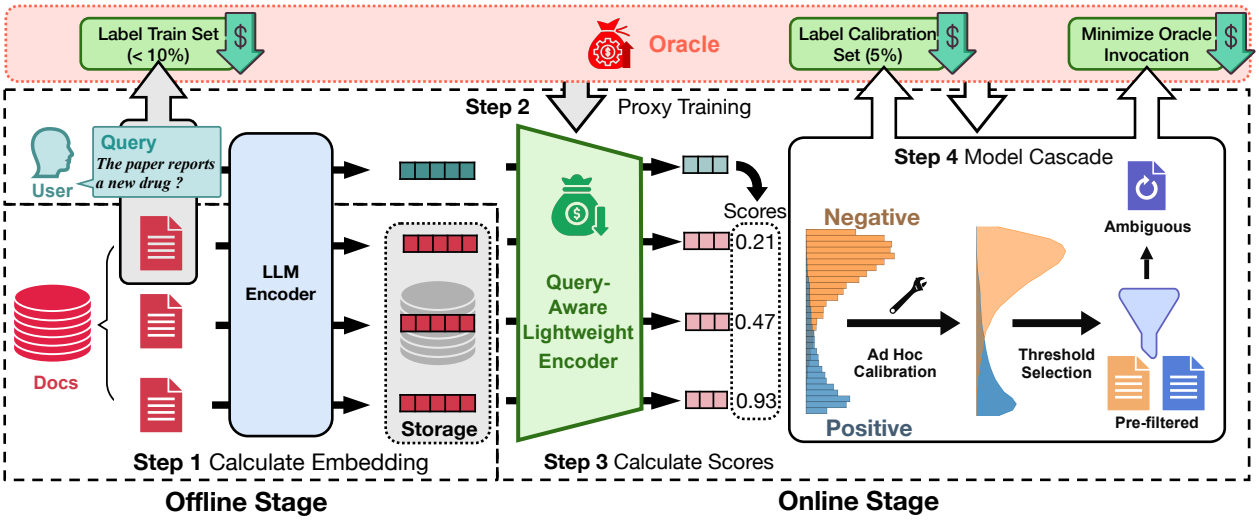

Figure 1: A detailed workflow of ScaleDoc – ScaleDoc efficiently adapts pre-computed embedding semantics for query-specific online processing, through its offline-online structure. The online process comprises a query-aware lightweight encoder and a subsequent cascade workflow.

online. Therefore, the second challenge is to design an efficient online calibration mechanism that can dynamically determine the effective thresholds, ensuring the final accuracy target is met with minimal oracle overhead.

To address these challenges, ScaleDoc introduces a novel contrastive learning based approach to train a robust proxy model (Section 3) and propose an efficient calibration workflow for the model cascade (Section 4). Together, these contributions ensure both high data reduction and robust accuracy for ad-hoc semantic predicates.

3 QUERY-AWARE MODEL TRAINING

The online efficiency of ScaleDoc hinges on a lightweight, Query-Aware proxy model. For each ad-hoc query, this model is trained to emulate the semantic judgments of the LLM oracle. It takes pre-computed document representations as input and outputs a decision score for each document, indicating the likelihood of satisfying the semantic predicate. This scoring enables a cascaded filtering process: high-confidence positive and negative documents are filtered, while only low-confidence, ambiguous documents are sent to the LLM oracle. Therefore, these decision scores, used to reduce the oracle invocations, are paramount to the overall system performance.

However, training a lightweight proxy model to produce effective decision scores is non-trivial. Basic approaches, such as the naive binary classifiers used in prior work [27, 39], struggle to capture query-specific semantics. Our preliminary experiments with a more advanced query-fused regression MLP also yielded unreliable scores.

To address this, we argue that the training process must be explicitly designed to produce scores with a well-behaved statistical distribution. We achieve this through a contrastive learning framework. In Section 3.1, we detail the desirable properties of this score distribution. Section 3.2 then describes how ScaleDoc leverages our contrastive learning mechanism to generate effective decision scores.

3.1 Desirable Distribution on Decision Scores

The primary goal of the lightweight model is to achieve effective data reduction, filtering more documents based on their decision scores. For clarity, we assumes a score distribution where higher scores indicate a higher likelihood of being positive and lower scores indicate being negative. Therefore, the low-score and high-score thresholds decide the results of pre-filtering.

In practice, achieving a high data reduction rate is not always guaranteed. Figure 2a exemplifies such a scenario, illustrating how a poorly-structured score distribution (*logprobs* of Llama-3.2-3B [9]'s first response token) can severely hinder data reduction. Specifically, the real positive class exhibits two peaks, appearing in both high and low score ranges. The attempt to set a filter threshold in the low-score region (e.g., the left red line) would misclassify many positives, violating the accuracy target and forcing a more conservative (and less effective) threshold. In contrast, Figure 2b illustrates a desirable distribution, showing a clear separation. Only minimal positive items fall below the red line threshold, allowing effective filtering of the true negatives.

To consistently achieve such effective data filtering, we propose three essential properties for the decision scores:

1) Smoothness. The distribution of decision scores should be continuous and smooth, without abruptions or discontinuities. This ensures that threshold-selection algorithms can operate stably and consistently. We have observed that this fundamental property fails with some naive proxies such as Kernel Density Estimation.

2) Semantic monotonicity. A document that is more semantically satisfying the query should be assigned a higher decision score, and vice versa. This prevents reward-hacking of deterministic score ranges, ensuring a meaningful and reliable ranking.

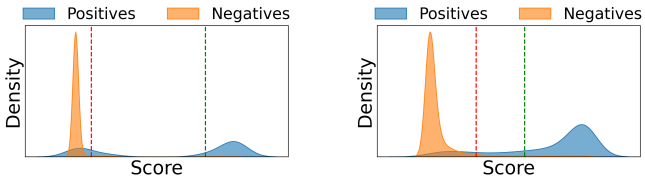

(a) Llama-3.2-3B logprobs **(b) ScaleDoc**

Figure 2: Example score distributions of different lightweight proxies with low and high data reduction rate.

3) Bipolarity. The score distribution must be strongly polarized, with positive and negative documents clustering distinctly at the high and low ends of the score spectrum. This clear separation is the primary driver of high data reduction.

Achieving these desirable properties is challenging. Compared to naive text classifier, our system leverages LLM-based embeddings, offering much richer semantic information. However, these embeddings are static and not optimized for the specific semantic distinctions of an ad-hoc query. Thus, directly training a lightweight model (e.g., MLP) on these embeddings typically results in inconsistent score distributions, failing to exhibit the vital properties. To overcome this challenge, the model needs to discover the discriminative query-specific patterns. We employ a contrastive-learning-based approach, which excels at learning fine-grained, task-specific distinctions.

3.2 A Contrastive Learning-based Approach

To instill the desired properties into the decision scores, ScaleDoc employs a contrastive learning framework. Contrastive learning [5] has a widespread adoption for bridging semantic gaps, particularly in scenarios where upstream representation learning tasks are not directly aligned with downstream applications. Therefore, it naturally fits into ScaleDoc's objective of transferring upstream raw embeddings to scores tailored for efficient model cascade. The core of this framework is a lightweight encoder $E(\cdot)$, which utilizes the MLP structure, mapping both the document and query into a shared **latent space**. To train the encoder for an ad-hoc query, we heuristically sample a small subset of documents (e.g., 5%) and use the oracle LLM to generate ground-truth labels (more details in Section 5).

Following this, the final decision score is constructed as the cosine similarity between the learned representations of the query and documents. This score is inherently smooth, and through our tailored training, is optimized to be both monotonically semantic and bipolar.

Formally, let q be a query and d be a document. We first obtain their high-dimensional semantic embeddings from a powerful LLM encoder, denoted as $\mathbf{e}_q \in \mathbb{R}^D$ and $\mathbf{e}_d \in \mathbb{R}^D$ respectively. ScaleDoc then employs a lightweight encoder, $E(\cdot) : \mathbb{R}^D \to \mathbb{R}^l$, mapping these embeddings into a latent space $\mathbb{R}^l$:

$$\mathbf{z}_q = E(\mathbf{e}_q), \quad \mathbf{z}_d = E(\mathbf{e}_d)$$

The decision score, $s(q, d)$, for the query-document pair is defined as the cosine similarity between their latent representations:

$$s(q, d) = \text{sim}(\mathbf{z}_q, \mathbf{z}_d) = \frac{\mathbf{z}_q \cdot \mathbf{z}_d}{\|\mathbf{z}_q\|\|\mathbf{z}_d\|}$$

A workload W consists of a query q and a collection of documents $\mathcal{D} = \{d_1, d_2, \ldots, d_N\}$. The complete set of decision scores for this workload can be expressed as::

$$S(W) = S(q, \mathcal{D}) = \{s(q, d_i) \mid d_i \in \mathcal{D}\}$$

To effectively shape the latent space and meet the required properties, ScaleDoc trains the encoder in two distinct phases. This two-phase strategy is crucial because jointly optimizing all properties simultaneously can lead to conflicting training signals and results in observed performance decline. Phase 1 first establishes the correct semantic relationship as the foundation. Then Phase 2 refines the spectrum of the embedding space to create a clear separation between positive and negative document clusters. There are three objectives during the overall training process, depicted in Figure 3.

Training Phase 1: Semantic Monotonicity The primary goal of Phase 1 is to build the foundational semantic relationship between the documents and the query predicate. To achieve this, we use a contrastive loss, $\mathcal{L}_{qsim}$, inspired by Dense Passage Retrieval (DPR) [17]. In our training, the query embedding $\mathbf{z}_q$ acts as an anchor. The objective is to pull positive document embeddings (d^+) closer to the anchor while pushing negative ones (d^-) away in the latent space.

A crucial distinction from DPR is that we train our encoder dynamically for each new query. This allows the model to learn query-specific semantics rather than a single, general-purpose matching function. This approach is essential in our setting; because our online proxy model is intentionally lightweight for efficiency, it lacks the capacity of the massive encoders used in DPR. By specializing the model for each query, we enable it to perform effectively despite its limited size, as shown in Figure 3(a).

Given a query q, each input mini-batch comprises m positive documents $\{d_i^+\}_{i=1}^m$ and $n-m$ negative documents $\{d_j^-\}_{j=1}^{n-m}$. The training loss is defined as

$$\mathcal{L}_{qsim}(q, \{d_i^+\}_{i=1}^m, \{d_j^-\}_{j=1}^{n-m}) = -log \frac{\sum_{i=1}^{m} e^{\text{sim}(q,d_i^+)/\tau}}{\sum_{j=1}^{n-m} e^{\text{sim}(q,d_j^-)/\tau} + \sum_{i=1}^{m} e^{\text{sim}(q,d_i^+)/\tau}} \quad (1)$$

Here, τ is a temperature hyperparameter. The optimization objective leverages the negative log-likelihood of the positive documents. It maximizes the likelihood of high similarity score between the query and positives while penalizing high similarities with negatives.

The training objective behind $\mathcal{L}_{qsim}$ results in query-direction ranking in the latent space through learned relocation. In the resulting manifold, the positive documents tend to appear near the query.

However, this phase alone is insufficient to guarantee the robust bipolarity property. While it correctly ranks documents relative to the query, it does not explicitly enforce a large separation margin

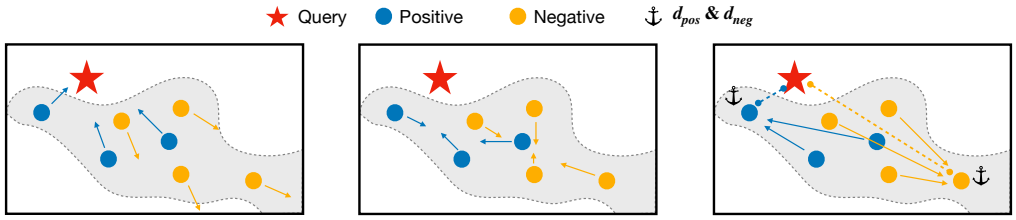

(a) $\mathscr{L}_{qsim}$ (b) $\mathscr{L}_{supcon}$ (c) $\mathscr{L}_{polar}$

Figure 3: Illustration of the objectives adopted in training ScaleDoc's Query-Aware Encoder.

between the entire positive and negative sets. Our observations indicate when relocation mappings are applied, local neighbors (mixed positive and negative instances) can move together, leading to a collapse of two classes into insignificant location relationships. This overlapping in score distribution hinders effective data filtering.

Training Phase 2: Enforcing Bipolarity To address the limitations of Phase 1, the second phase explicitly shapes the latent space to form a bipolar distribution. Using the same encoder and training data, we introduce two loss functions, $\mathcal{L}_{supcon}$ and $\mathcal{L}_{polar}$.

First, aligned with the Supervised Contrastive Learning [19], $\mathcal{L}_{supcon}$ encourages intra-class clustering. It pulls documents of the same label together, forming tight clusters. For each document d_i in a mini-batch, intra-class instances are pulled closer while those with different labels are pushed further apart, as shown in Figure 3(b).

$$\mathcal{L}_{supcon}(\{d_i\}) = -\sum_{i=1}^{n} \frac{1}{|U(i)|} \log \frac{\sum_{d_p \in U(i)} e^{\text{sim}(d_i,d_p)/\tau}}{\sum_{d_k \in A(i)} e^{\text{sim}(d_i,d_k)/\tau}} \quad (2)$$

where $U(i)$ denotes documents sharing the same label with d_i, and $A(i)$ is the set of all other documents in the mini-batch besides d_i. The optimization is performed upon the average of all documents' negative log-likelihood. For all documents inside each mini-batch, it fosters its similarity to other documents of the same label, relative to similarity with all other documents. Therfore, this objective significantly contributes to bipolarity by minimizing the variance within each class.

Second, $\mathcal{L}_{polar}$ introduces a novel mechanism to explicitly enforce a bipolar manifold and enlarge the margin between classes. The intuition behind $\mathcal{L}_{polar}$ is selecting a *bellwether* sample for positives and negatives in each mini-batch to guide the direction of clustering. A bellwether is distinguished by the closest (positive) or furthest (negative) distances relative to the query inside each mini-batch. For a given mini-batch and query, we define the bellwethers as:

$$d_{pos} = \underset{d_i \in \{d^+\}}{\text{argmin}}\ \text{sim}(q, d_i), \quad d_{neg} = \underset{d_j \in \{d^-\}}{\text{argmax}}\ \text{sim}(q, d_j)$$

$\mathcal{L}_{polar}$ then uses these bellwethers as anchors, pulling all positive documents towards d_{pos}, and and all negative documents towards d_{neg}.

$$\mathcal{L}_{polar}(q, \{d_i^+\}_{i=1}^{m}, \{d_j^-\}_{j=1}^{n-m}) = -(log \frac{\sum_{i=1}^{m} e^{sim(d_{pos},d_i^+)/\tau}}{\sum_{j=1}^{n-m} e^{sim(d_{pos},d_j^-)/\tau} + \sum_{i=1}^{m} e^{sim(d_{pos},d_i^+)/\tau}} + log \frac{\sum_{i=1}^{n-m} e^{sim(d_{neg},d_i^-)/\tau}}{\sum_{j=1}^{n-m} e^{sim(d_{neg},d_j^-)/\tau} + \sum_{i=1}^{m} e^{sim(d_{neg},d_i^+)/\tau}}) \quad (3)$$

Bellwethers can be different across mini-batches, but $\mathcal{L}_{polar}$ ensures a consistent relocation. The progressive process explicitly enlarges the separation margin between the positive and negative poles. This constructs a highly bipolar manifold, enhancing the efficacy of threshold-based filtering, as shown in Figure 3(c).

Collectively, these two training phases and three loss functions effectively shape the latent space to produce effective decision scores, satisfying our proposed properties. Section 6.4 show more details about our experimental evaluation.

4 MODEL CASCADE

After the lightweight proxy procedure, ScaleDoc uses a powerful but expensive LLM oracle to resolve uncertain predictions through its model cascade component. Model cascade aims to meet the user-specified accuracy target while minimizing oracle invocations by filtering out most documents based on the proxy model's scores and only forwarding the most ambiguous cases to the oracle.

In ad-hoc settings, the lack of prior knowledge about query-specific labels and data distribution poses a significant challenge for model cascades, often leading to suboptimal data reduction in existing methods [16]. ScaleDoc addresses this by introducing a novel calibration workflow and optimized filtering algorithm. By leveraging the well-behaved decision scores from our lightweight model (Section 3), ScaleDoc achieves superior data reduction while robustly meeting accuracy targets.

This section proceeds as follows. Section 4.1 formulates the cascade task as a constrained optimization problem. Section 4.2 introduces our ad-hoc calibration method, which enables accurate performance estimation from a small, sampled subset of data. Section 4.3 details the algorithm for selecting optimal filtering thresholds to solve the optimization problem.

4.1 Problem Formulation

For a given query, the lightweight proxy model produces a decision score for each document, denoted by $S(W)$, a cosine similarity within the interval $[0, 1]$. Recall that a higher score indicates a stronger semantic agreement with the query. To filter out the high-confidence instances, the cascade component should select two thresholds, a lower bound lb and an upper bound rb. The filtering logic is as follows:

- Documents with scores in $(rb, 1]$ are classified as **positive**.
- Documents with scores in $[0, lb)$ are classified as **negative**.
- Documents with scores in $[lb, rb]$ are deemed **ambiguous** and are sent to the LLM oracle for final decision.

The primary goal is to minimize the fraction of documents sent to the LLM oracle, while satisfying the user-specified accuracy target α. We define this fraction as the unfiltered rate, u, which is controlled by the lower bound and upper bound:

$$u(lb, rb) = \frac{|\{s_i \in S(W) \mid lb \le s_i \le rb\}|}{|S(W)|} \tag{4}$$

The final accuracy of our framework, $\text{Acc}(lb, rb)$, is determined by the correctness of the lightweight model in the filtered regions, combined with the perfect accuracy of the oracle on the unfiltered region $[lb, rb]$.

This leads to the following constrained optimization problem, where $\mathcal{K}$ represents the valid search space for (lb, rb), with $0 \le lb \le rb \le 1$.

$$\min_{(lb,rb)\in\mathcal{K}} u(lb, rb) \quad \text{s.t. } \text{Acc}(lb, rb) \ge \alpha \tag{5}$$

Solving this problem in an ad-hoc setting is challenging, because the function $\text{Acc}(lb, rb)$ is unknown without full ground truth statistics. Therefore, a calibration process is required to estimate the accuracy, followed by the thresholds selection for pre-filtering.

4.2 Ad-hoc Calibration

To solve the optimization problem of cascade (i.e. Equation 5), we must obtain the accuracy $\text{Acc}(lb, rb)$ for any given threshold pair (lb, rb). However, in the ad-hoc setting, accurate labels for the entire document collection are unavailable. Therefore, ScaleDoc relies on a small, oracle-labeled sample to estimate the accuracy and calibrate the cascade process. Formally, from the full set $S(W)$, a subset $S'(W)$ is sampled and labeled.

This approach, however, introduces a critical challenge: a small sample may fail to capture the global relationship between the accurate labels and the proxy scores $S(W)$. Specifically, the sampled score distributions can deviate significantly from the true global distributions. This discrepancy can lead to poorly calibrated threshold (lb, rb), which fails to meet the global accuracy target. The pitfall can be attributed to two main failures: 1) simple random sampling might under-represent documents in low-density score regions or *information loss*, especially in *tail* regions, and 2) sample randomness introduces stochastic noise. While a sufficiently large large sample set could mitigate this estimation bias, the associated cost of oracle labeling is prohibitive.

Algorithm 1 Ad-hoc Calibration Workflow

Given: Decision scores $S(W)$, Oracle LLM
$bins \leftarrow \text{Discretize}(S(W))$ ▷ Discretize score range into bins for stratified sampling and analysis
$S'(W) \leftarrow \text{StratifiedSample}(S(W))$ ▷ Sample representatively from each partition
$S'_P \leftarrow \{s_i \mid s_i \in S'(W) \wedge \text{Oracle}(q, d_i) = \text{positive}\}$
$S'_N \leftarrow \{s_i \mid s_i \in S'(W) \wedge \text{Oracle}(q, d_i) = \text{negative}\}$
$PDF_P \leftarrow \text{Smooth}(\text{DE}(\text{Jitter}(S'_P)))$ ▷ Reconstruct score distribution for positive class
$PDF_N \leftarrow \text{Smooth}(\text{DE}(\text{Jitter}(S'_N)))$ ▷ Reconstruct score distribution for negative class
return $PDF_P, PDF_N, bins$

To address this, ScaleDoc introduces a robust calibration workflow. This workflow, detailed in Algorithm 1, accurately reconstructs the global score distributions for positive and negative documents from a small sample. It comprises two main stages: **stratified sampling** and **distribution reconstruction**. Our experiments demonstrate that with a modest sample size of 5%, ScaleDoc can achieve substantial data reduction while satisfying the accuracy constraint.

Stratified Calibration Sampling. Uniform random sampling can lead to two common limitations. First, it fails to capture the distribution of scores in low-density score regions, as being studied in [16]. Second, random noise can invalidate sampled distribution by introducing heterogeneity and bias, especially with smaller sample sizes.

To address these issues, we propose to employ stratified sampling. We discretize the entire score range into a series of bins. Then, we sample from each bin in proportion to its population in the global set $S(W)$. This ensures that the sampled subset $S'(W)$ preserves the relative density of the global distribution, preventing low-density regions from being entirely omitted.

Distribution Reconstruction. After obtaining the labeled sample $S'(W)$, we reconstruct continuous and robust score distributions for positive and negative instances. The core objective is to faithfully mirror the global distributions $S(W)$, optimized through the following mathematic process:

1) Jittering for Information Recovery. To counteract information loss, especially in low-density regions, we first apply random jittering. Stratified sampling with a modest rate can cause bins with few samples to become empty. Ignoring these gaps encourages overconfidence in these score ranges, creating a risk factor for failing accuracy targets in subsequent threshold selection. Jittering addresses this by introducing low-density, random data into these empty bins, ensuring that this information is not lost before subsequent modeling.

2) Density Estimation (DE) via Linear Interpolation. Next, we construct the continuous Probability Density Functions (PDF_P and PDF_N) from the discrete, jittered samples. We employ *linear interpolation* for this density estimation task, providing a virtually distortion-free modeling. This process yields a continuous probabilistic interface that facilitates subsequent accuracy calculations via density integration rather than discrete sample counting. This

Algorithm 2 Thresholds Selection

Given Reconstructed CDF_P, CDF_N; discretization *bins*
steps ← *bins.edges* ▷ Initialize thresholds search space to be edges from discretization
l_s, r_s ← *steps*.first, *steps*.last
function SelectThresholds (α)
    $l_0, r_0 \leftarrow l_s, r_s$ ▷ Initialize thresholds
    ▷ 1. Find the tightest l_0 with $r = r_s$
    for l **from** *steps.first* **to** *steps.last* **do**
        if $\text{Acc}(l, r_s) \geq \alpha$ **then** $l_0 \leftarrow l$ **else break**
    end for
    ▷ 2. Find the tightest r_0 with $l = l_s$
    for r **from** *steps.last* **to** *steps.first* **do**
        if $\text{Acc}(l_s, r) \geq \alpha$ **then** $r_0 \leftarrow r$ **else break**
    end for
    ▷ 3. Construct frontier path P from (l_0, r_s) to (l_s, r_0)
    $l, r \leftarrow l_0, r_s$
    $P \leftarrow \{(l_0, r_s)\}$
    while $(l, r) \neq (l_s, r_0)$
        $l_{next}, r_{next} \leftarrow l + bins.size, r - bins.size$
        if $\text{Acc}(l_{next}, r) \geq \alpha$ **then**
            $l \leftarrow l_{next}$
        else
            $r \leftarrow r_{next}$
        $P \leftarrow P \bigcup \{(l, r)\}$
    ▷ 4. Find the best threshold pair on the path P
    $l_t, r_t \leftarrow \underset{(l,r)\in P}{\text{argmin}}\ \text{Unfiltered}(l, r)$
    return l_t, r_t

allows querying over arbitrary scores for an estimated density value. Compared to methods like Kernel Density Estimation (KDE), linear interpolation provides a more faithful representation of the empirical distribution, particularly in low-density regions.

3) Smoothing. Finally, to mitigate anomalous noise and information loss from sampling randomness, we apply the Moving Average (MA) approach. MA is a simple soft computing method that smooths the distribution by applying mean pooling within a fixed-size sliding window, which allows for a better capture of the general distributional features. Applying an MA filter reduces spikes and breakpoints, providing an additional layer of smoothing to reveal the underlying global trend more effectively.

With the above optimizations, the reconstructed distributions serve as a continuous and robust foundation for the subsequent threshold selection process. The final outputs of Algorithm 1 are the distributions of positives and negatives in the form of PDFs, and the discretization of the score range *bins*.

4.3 Threshold Selection

After reconstructing the score distributions through calibration, the final step is to select the optimal threshold pair (lb, rb) that solves the optimization problem defined in Equation 5. The goal is to minimize the unfiltered rate $u(lb, rb)$ while satisfying the user-specified accuracy target α.

A basic brute-force search over all possible threshold pairs (l, r) is computationally infeasible, having a quadratic time complexity with respect to the number of possible threshold values. To overcome this, we introduce an efficient algorithm that leverages the monotonic properties of the calibrated score distributions. The core insight is that any optimal solution must lie on the Pareto-frontier of the feasible set defined by the accuracy constraint, $\text{Acc}(l, r) \geq \alpha$. Any point not on this frontier is suboptimal and its unfiltered rate can be improved, by tightening the thresholds and moving towards the frontier, without violating the accuracy constraint.

Our approach, presented in Algorithm 2, efficiently finds this optimal pair by systematically tracing the frontier. The potential thresholds, denoted as *steps*, are discrete bin boundaries in our calibration sampling. The algorithm proceeds in three main phases:

1) Boundary Identification: Ensuring the accuracy target, the algorithm first determines the two extreme points of the feasible frontier: (l_0, r_s) and (l_s, r_0). Here, l_0 is the tightest (highest) lower bound possible when the upper bound is most conservative (r_s), and r_0 is the lowest upper bound when the lower bound is most conservative (l_s). This step effectively bounds the search space to a one-dimensional path.

2) Frontier Traversal: Starting from (l_0, r_s), the algorithm iteratively constructs a path P that approximates the feasible frontier. It greedily moves towards the other extreme point (l_s, r_0) by tightening either l or r at each step, ensuring the accuracy constraint α is never violated.

3) Optimal Point Selection: Since the unfiltered rate $u(lb, rb)$ is monotonically decreasing with respect to the size of the filtered region, the optimal point that minimizes u must lie on the path P. The algorithm simply evaluates $u(l, r)$ for all points on P and returns the pair (l_t, r_t) that yields the minimum value.

This algorithm reduces complexity from quadratic to linear with respect to the number of discretization steps. Due to space constraints, we present only an intuitive overview here; formal proofs of optimality will be provided in an extended version.

5 IMPLEMENTATION DETAILS

We implemented ScaleDoc using Python and PyTorch. Our implementation automates the entire pipeline, including data sampling, ground-truth labeling, model training, calibration, and the final cascade filtering. This section discusses several key design decisions and optimizations within the system.

Training Set Materialization. In the online phase, the initial step is to sample a small training set from the document collection and obtain ground-truth labels from the oracle. However, ad-hoc queries often exhibit significant variance in selectivity, especially for rare conditions that match few documents. Training on such imbalanced datasets can hinder the model's ability to learn the discriminative features of the minority class, resulting in a biased and ineffective proxy.

To address class imbalance, we implement a fallback-style rebalancing method. After labeling an initial random sample, we check the positive-to-negative ratio. If the minority class has too few examples, we augment the data by adding Gaussian noise to the

existing minority class embeddings and assigning them the corresponding label, thus creating a more balanced training set for the proxy model.

Model Training. The proxy model's encoder, $E(\cdot)$, is a 3-layer perceptron (MLP). It takes the embeddings as input and maps them into a latent space. Following standard practice in contrastive learning [5, 10], we append a secondary MLP, the projector head $Proj(\cdot)$, after the encoder during the training phase. This projector head is discarded during inference. To train our encoder, each mini-batch is constructed with embeddings of multiple documents alongside the single query embedding. This forces the encoder to optimize the shared latent space representations for both adaptively, distinguishing our approach from conventional methods.

As defined in Section 3.2, Training Phase 2 optimizes a joint loss function: $\mathcal{L}_2 = \lambda \cdot \mathcal{L}_{supcon} + (1-\lambda) \cdot \mathcal{L}_{polar}$. The hyperparameter λ balances the two losses. Across all experiments, we empirically set $\lambda = 0.2$. We found that the system's performance is not sensitive to this parameter, and extensive tuning did not yield significant improvements.

Model Cascade. A critical parameter in the calibration step is the discretization granularity, which determines the number of bins used to partition the proxy model's score range (i.e., the *steps* variable in Algorithm 2). The choice of discretization granularity involves a trade-off: too few bins may inaccurately approximate the global score distribution, while too many bins can result in unrepresentative samples due to insufficient data points per bin. Empirically, we set the granularity to 64, which provides a robust balance for capturing distribution shapes across diverse datasets and queries.

6 EVALUATION

We evaluated ScaleDoc against various baselines across diverse workloads, where ScaleDoc consistently outperformed all baselines in end-to-end performance. We then conducted further experiments to demonstrate the performance trade-off and the individual contributions of two major components (i.e., query-aware proxy model and ad-hoc cascade mechanism). Finally, we discussed different hyperparameter configurations within our system.

6.1 Experiment Setup

Workloads. Each experimental workload is defined by a tuple: (*query, document collection, accuracy target*). To evaluate performance across diverse settings, we use three real-world document collections: BigPatent [37], PubMed [7], and GovReport [12]. Given the lack of benchmarks for collection-level semantic predicates, we manually crafted 20 distinct natural-language queries for each collection, covering a wide range of semantic characteristics and data selectivity. Each collection contains 10,000 documents, and the ground-truth labels for all query-document predicating pairs are generated using GPT-4o. Table 1 provides a summary of the datasets and illustrative queries.

Baselines. We compare ScaleDoc against several representative baselines, which accelerate the ML-powered predicates in analytical data systems. The oracle model for all systems, which also serves as the ground truth labeler, is **GPT-4o** [30].

1) Oracle Only. This baseline avoid any filtering and processes every document directly using the oracle LLM. We prompt the LLM to output the binary class labels to indicate the predicating decision.

2) Probabilistic Predicates (PPs) [27, 39]. This approach uses traditional lightweight machine learning models as proxies. For each new problem, the PPs are trained to output binary classification results with confidence interface. It includes the following compoent choices:

- Text Representation: Bag-of-Words (BoW) and TF-IDF, both are standard text encoding schemes.
- Dimensionality Reduction: Principal Component Analysis (PCA) and Feature Hashing (FH).
- Classifier: Support Vector Machines (SVM) and Kernel Density Estimation (KDE).

These models are implemented using Scikit-learn. We explore various combinations of these compoents and reporting the best-performing choices.

3) LLM Cascade [4, 31]. This method employs smaller LLMs as proxies, a common strategy in recent works. We use vLLM engine [20] for optimized, low-latency inference. The proxy LLM is prompted to classify a document against the query and provide a confidence score based on the log probabilities of the output token. We evaluate several configurations as follows:

- **Llama-3.2-1B + Oracle**: A single-stage cascade using Llama-3.2-1B [9] as the proxy.
- **Llama-3.2-3B + Oracle**: A similar setup with a 3B model. It takes up more computation for inference, but produce better predictions.
- **Llama-3.2-1B + Llama-3.2-3B + Oracle**: A two-stage cascade that uses the 1B model to filter for a the 3B proxy, which in turn filters for the oracle.

4) ScaleDoc (ours) For the offline representation phase, we use NvEmbed [21], derived from Mistral-7B [14], to pre-compute the document embeddings. In the online phase, our lightweight proxy model is implemented as a 3-layer MLP.

Experimental Details. Each workload operates on a collection of 10,000 documents. For methods requiring a proxy (i.e., ScaleDoc and PPs), we sample approximately 1,000 documents (10%), used for training and calibration. The remaining 9,000 documents are then processed online. Baselines that do not require training (i.e., oracle-only and LLM-cascade) just process the entire collection online. Lightweight model inference was executed on the NVIDIA A10 GPU. The oracle (GPT-4o) was accessed via the Azure-OpenAI API, subject to a rate limit of 150k tokens per minute.

6.2 End-to-End Performance

We evaluate end-to-end online performance of ScaleDoc against mentioned baselines. Figure 4 presents the average online latency and data reduction for each system across three datasets, with a user-specified accuracy target of $\alpha = 0.90$. α for all the latter experiments will be 0.90 if not specified. The results show that ScaleDoc consistently and significantly outperforms all other approaches, achieving an average online **speedup over 2×**. And reduce the invocation of oracle LLMs up to **85%**, which means the **6.6× cost-saving**. This performance gain is driven by our effective data filtering methods and the computational efficiency of our lightweight design.

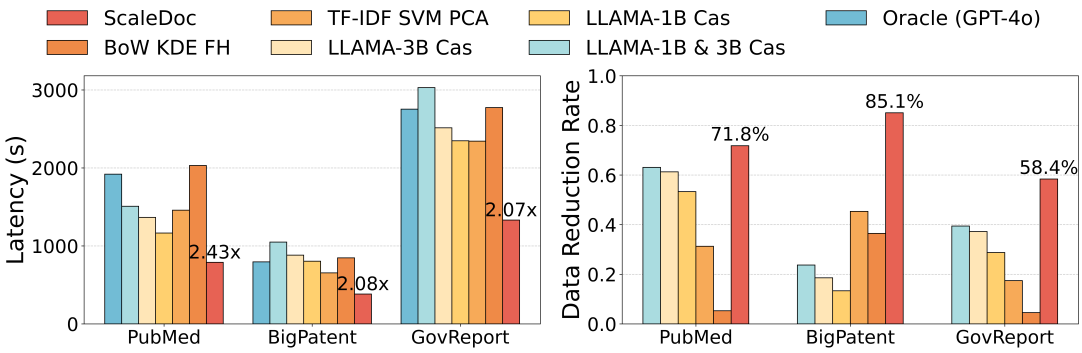

Figure 4: End-to-end latencies and data reduction rate – We evaluate ScaleDoc and other baselines with accuracy target $\alpha = 0.90$. The data reduction rate measures the percentage of data that does not require the LLM oracle call, indicating the cost-saving.

Table 1: Dataset Characteristics

Dataset	Content	Avg. Word Count	Example Query
PubMed	Abstracts from medical papers	413	Report efficacy of a certain medicine?
BigPatent	Summaries on U.S. patent documents	129	Introduce inventions of cross-sectional technology?
GovReport	Reports from government	621	About environment protection?

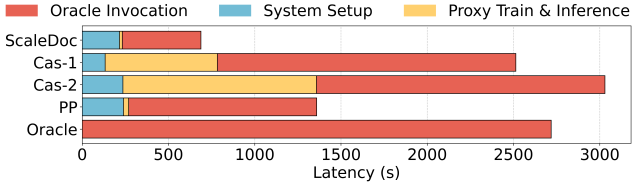

Figure 5: Breakdown for different pipelines, measuring average latencies in each stage of the pipelines. – Oracle shows the estimated latency of a single pass of oracle inference through all the documents.

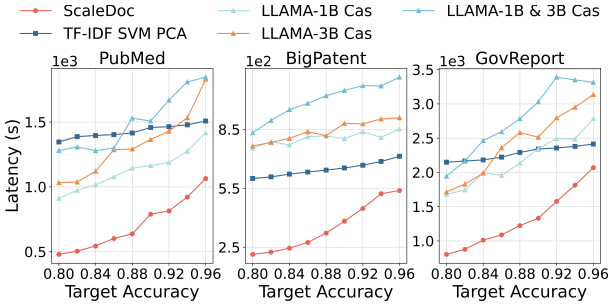

Figure 6: Accuracy-Latency tradeoff on three datasets.

To provide a granular performance analysis, Figure 5 breaks down the average latency of each online processing stage from workloads based on PubMed. This breakdown accounts for initial setup costs, such as ground truth labeling for proxy training and calibration. We can observe that beyond ScaleDoc's substantial reduction in oracle LLM invocations, its efficiency is also driven by its lightweight proxy model, both for the training and inference. In contrast, the LLM cascade methods (Cas-1, Cas-2) exhibit a critical performance bottleneck. Although their proxy models (smaller LLMs) offer training-free zero-shot capabilities, they still incur prohibitive computational costs during inference, leading to high end-to-end latency. Surprisingly, a traditional approach (e.g., TF-IDF with an SVM classifier), despite its general-purpose limitations, can outperform LLM cascades after adaptive training and tuning, thanks to its lower online computational cost.

Offline Overhead ScaleDoc needs an offline computation for document representation, but this overhead is small. Encoding 10,000 PubMed documents with NvEmbed is a **one-time** process requiring about 24 PFLOPs, according to [42]. Conversely, during online processing, an LLM oracle like Llama-3-70B [9] (comparable to GPT-4o) demands 10× more computation for each ad-hoc query. Even a lightweight proxy model such as Llama-3.2-3B uses 13 PFLOPs per query, a cost incurred every time. This highlights that ScaleDoc's one-time offline overhead is comparatively small and acceptable.

6.3 Accuracy-Latency Tradeoff

We evaluated the accuracy-latency trade-off by setting accuracy targets from 0.80 to 0.96. As shown in Figure 6, ScaleDoc consistently reduces average runtime across all three datasets and accuracy targets. And all the methods exhibit a common trend: higher accuracy targets generally incur more online latency.

When accuracy targets are relaxed, ScaleDoc's latency decreases by a larger margin, offering more trade-off opportunities for higher performance. In contrast, other baselines show smaller latency variation, due to their unreliable decision scores, which lack semantic

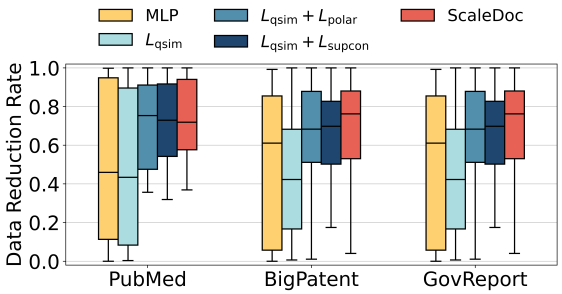

Figure 7: Pseudo end-to-end data reductions on different workloads – MLP trains a binary classifier MLP on document embeddings. $\mathcal{L}_{qsim}$, $\mathcal{L}_{supcon}$, $\mathcal{L}_{polar}$ are ablation-style variants of ScaleDoc's Query-Aware encoder.

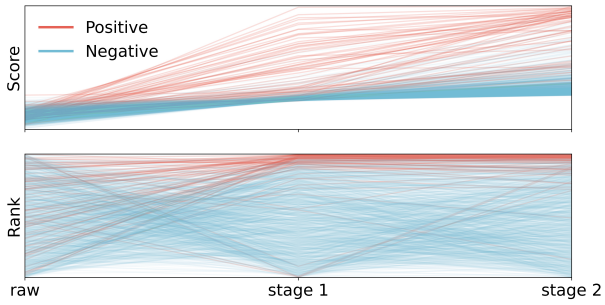

Figure 8: Embedding relocation mapping during Query-Aware training. – Score stands for the numerical values of cosine similarity scores, and Rank stands for the relative order of the scores. Each line demonstrates the relocation trace of a single document in the latent space throughout 2 training phases.

monotonicity and bipolarity. This limits their effectiveness of data reduction even with relaxed accuracy.

6.4 Impact of Query-Aware Model Training

In this section, we will validate the effectiveness of the Query-Aware training within ScaleDoc. We demonstrate how ScaleDoc's specialized training objective leads to superior data filtering.

Figure 7 illustrates the effectiveness of Query-Aware training through pseudo end-to-end data reduction results. The term *pseudo* signifies that a brute-force optimal cascade algorithm is applied, specifically to isolate the impact of the training framework from other cascade designs. The key findings are:

1) Superiority of Query-Aware Training. ScaleDoc significantly outperforms basic approach (i.e. directly training a MLP binary classifier), leading to a 20% average increase in data reduction. This improvement is particularly noticeable in *hard* cases, where the data reduction rates is inherently lower.

2) Effectiveness of different losses. Our ablation study reveals the distinct roles of the different loss functions. Using only $\mathcal{L}_{qsim}$ loss from Training Phase 1 seems to be ineffective. However, the inclusion of Training Phase 2, which incorporates $\mathcal{L}_{supcon}$ and $\mathcal{L}_{polar}$, remedies this issue and achieve the final performance. This does not diminish the role of $\mathcal{L}_{qsim}$. In fact, models trained without Phase 1 failed to produce valid results, demonstrating that establishing an initial semantic ranking is a fundamental prerequisite.

To gain deeper insights into the training objectives, we conduct further experiments as follows:

$\mathcal{L}_{qsim}$ guarantees semantic monotonicity. Figure 8 illustrates how the lightweight encoder transforms the document representations. Recall that the encoder learns a mapping from the original embedding space (Raw) to a new latent space, where scores reflect semantic consistency to the predicates. Initially, the positive and negative documents are intermingled. After Phase 1 training with $\mathcal{L}_{qsim}$, they become semantically orderly: positive documents are mapped to high-score regions and negatives to low-score regions. This establishes *semantic monotonicity*, providing a crucial foundation for the subsequent training.

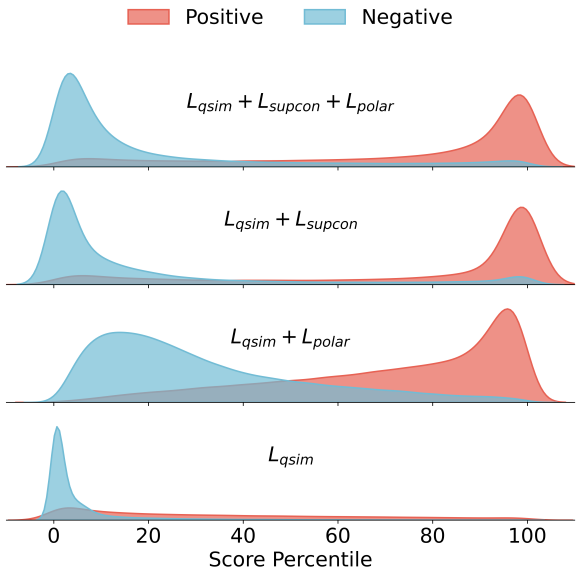

Figure 9: Average score distribution of positives and negatives – The four model variants are trained with different losses in an ablation style. All scores are normalized into percentiles.

$\mathcal{L}_{supcon}$ and $\mathcal{L}_{polar}$ creates bipolar distribution. Figure 9 shows the resulting score distributions with different training objectives. Training with $\mathcal{L}_{qsim}$ alone produces overlapping distributions for positive and negative documents, making it difficult to set a reliable filtering threshold. Both $\mathcal{L}_{supcon}$ and $\mathcal{L}_{polar}$ address this by creating a *bipolar distribution*, pushing positive and negative scores to opposite ends of the spectrum. Specifically, $\mathcal{L}_{supcon}$ is effective at clustering documents with the same label, creating *high-kurtosis peaks*. However, its drawback is the creation of small, incorrect sub-clusters in the tail regions. $\mathcal{L}_{polar}$, in contrast, does not cluster as aggressively, but is more effective at shaping the tails of the distributions. This creates a cleaner separation and mitigates the side effects of $\mathcal{L}_{supcon}$.

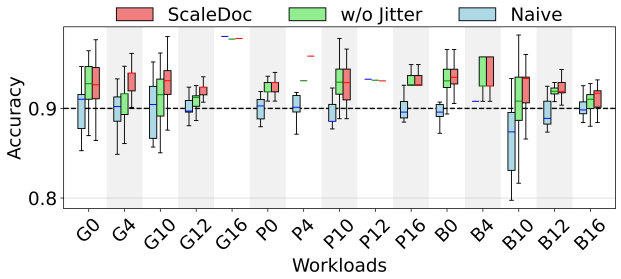

(a) Accuracy on 100 trials – Naive performs brute-force search in the search space on raw calibration set without distribution reconstruction. Black dotted line demonstrate accuracy target α=0.90.

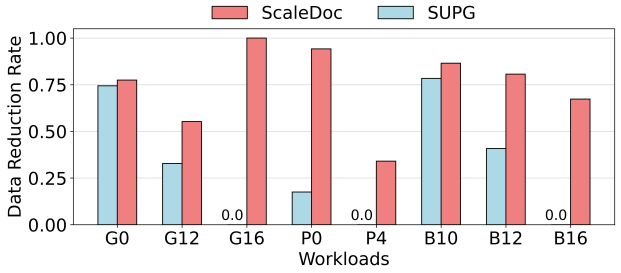

(b) Average data reduction

Figure 10: Zero-shot cascade accuracy and data reduction rate

6.5 Model Cascade Validation

Validate the Cascade Accuracy Ad-hoc cascade, often inherently lack prior knowledge to guarantee predefined accuracy targets. In Section 4.2, we highlight the importance of reconstructing the score distribution from a small calibration set. We validate the efficacy of this ad-hoc calibration workflow by testing pre-filtering for cascade for 100 trials on 15 workloads, using 5% of the data from stratified sampling. The naive approach (Naive) directly selects thresholds on the raw calibration set without distribution reconstruction and fails to meet the predefined accuracy target α in nearly half of the trials. This failure, discussed in Section 4.2, stems from the limited size of the calibration samples. As shown in Figure 10a, the ad-hoc calibration workflow we propose increases the likelihood of achieving the accuracy target, enabling ScaleDoc to meet α=0.90 in more than 80% of the trials, with a worst-case accuracy loss of only 0.04.

Comparison to SUPG SUPG is a common algorithm adopted in existing systems [16, 31] that leverages Importance Sampling and statistical bounds in thresholds selection. We implement SUPG following the interface [31] and compare it with ScaleDoc (Figure 10b). While SUPG offers theoretical performance guarantees, it often struggles to yield practically reasonable thresholds with modest calibration sets. In contrast, ScaleDoc's approach consistently outperforms SUPG across various workloads, demonstrating more reliable and generalized performance.

Validate Density Estimator The effectiveness of ad-hoc calibration relies on a faithful Density Estimator (DE) for the score distribution. A good DE should accurately model original distributions from a small subset. To validate its effectiveness, we leverage Jenson-Shannon Distance (JSD) to measure the discrepancy between the reconstructed distribution and the original full distribution. We compare the quality of ScaleDoc's DE results (SD) with other estimators, such as Importance Sampling (IS) and directly fitting Beta distribution curves (B). As shown in Table 2, across 10 different workloads, our DE (optimized with linear interpolation) achieves lowest discrepancy in general, ensuring the selected thresholds are accurately transferable to the full set.

Table 2: JSD between reconstructed distribution and ground truth (Lower is better). – N denotes Naive stratified sampling. p/n denotes positive and negative distributions.

	N-p	N-n	IS-p	IS-n	B-p	B-n	SD-p	SD-n
Mean	0.30	0.11	0.34	0.18	0.50	0.38	**0.20**	**0.09**
Median	0.32	0.08	0.33	0.17	0.42	0.43	**0.16**	**0.08**

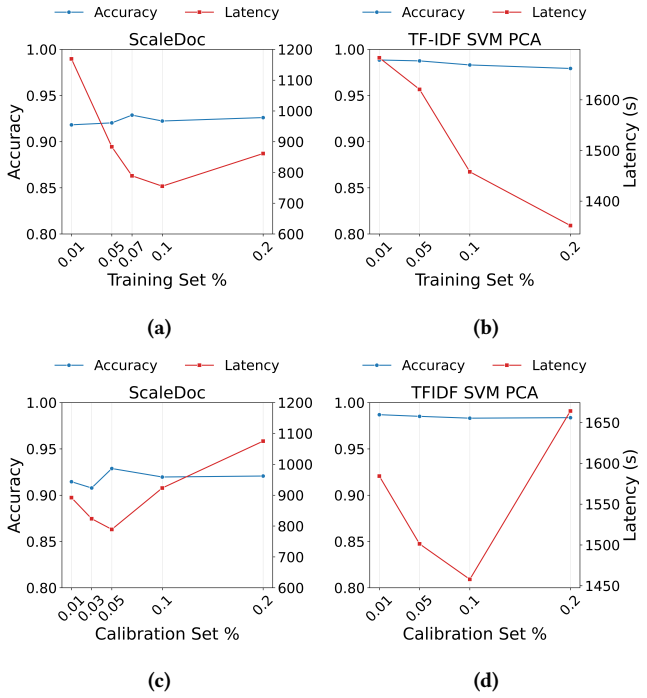

Figure 11: Accuracy and Latency with different hyperparameters. – Training Set % and Calibration Set % denotes the portion of data sampled from global for training and calibration, respectively.

6.6 Impact of Hyperparameters

The training and calibration set sizes in ScaleDoc are key hyperparameters. We demonstrate their impact on ScaleDoc's end-to-end performance with the target accuracy of 0.90 (see Figure 11). For the training set, larger sizes initially improve the proxy model's ability to learn global features, enhancing efficacy. However, this eventually led to increased labeling overhead and a higher latency.

The preferred trade-off is empirically found with a training set size between 7% and 10%. Conversely, a standard PP pipeline (i.e. TF-IDF SVM PCA) requires much more labels to train effectively, leading to more LLM oracle invocations. A similar trade-off exists for the calibration set. We show that a sample rate of 5% is sufficient to capture global score distributions without excessive labeling overhead, maximizing end-to-end performance.

7 RELATED WORK

In this section, we present a brief review on advances related to ScaleDoc and discuss how our contributions extend or differ from existing approaches.

LLMs in Data Systems The advent of Large Language Models (LLMs) has catalyzed a paradigm shift in data analysis, due to their remarkable zero-shot reasoning and instruction-following capabilities. For instance, numerous studies have explored using LLMs to translate natural language into SQL queries [23, 26, 28], effectively lowering the barrier to database interaction. And LLMs are also being integrated as agentic components to orchestrate complex data preparation and processing workflows [36, 40]. Furthermore, analytical systems such as Lotus [31] and Palimpzest [25] formulate *semantic operators*, which provide and integrate several declarative LLM interfaces over unstructured data. Other works target various essential tasks such as multi-class text classification [18], data cleaning [41], and entity extraction [11], exemplifying the versatility of LLMs. In parallel, ScaleDoc addresses the foundational and ubiquitous task of semantic predicate filtering. Our goal is to develop a general, scalable, and cost-effective solution for this primitive, which is critical for a wide range of analytical scenarios.

Acceleration for Machine Learning Queries The high computational cost of machine learning (ML) inference, particularly for LLMs, has made acceleration a critical area of research.

Some works focus on low-level architecture and hardware optimizations to accelerate LLM inference. For instance, PagedAttention [20] and FlashAttention [6] improve performance by optimizing the attention mechanism and memory access at the GPU level. Others optimize the scheduling of low-level execution engines, featuring DistServe [42] with disaggregated inference phases for better efficiency and Sarathi [1] segmenting extensive prefilling computation into aligned chunks. Our work is orthogonal to these approaches, focusing on a higher layer of the analytical system stack.

At the higher system level, to accelerate the ML-powered queries, recent works demonstrate the emergence of the proxy-cascades workflow. In this paradigm, a lightweight proxy model rapidly filters out easy entities before sending to a powerful, expensive model. For instance, Probabilistic Predicates (PPs) [27, 39] employed simple classifiers or density estimators as pre-filtering proxies. Similarly, NoScope [15] built a cascade system to accelerate object detection in video databases. More recently, with the advent of LLMs, systems like FrugalGPT [4] and Palimpzest [25] have adapted the design of using smaller LLMs as proxies for more powerful ones. However, these approaches often show limited performances in the face of ad-hoc queries. Specifically, PP-based proxies and NoScope lack generalizability to new workload patterns, demanding costly re-training the proxies. LLM-centric solutions still depend on the capability of costly, moderate-scale LLM proxies. Our work addresses these limitations by exploring a more generalizable, lightweight, and automated solution for semantic queries, advancing reliable acceleration.

Semantic Representation Semantic representations, which encode the meaning of text into dense vectors, are foundational to a myriad of Natural Language Processing (NLP) applications [33]. Early advancements, such as Sentence-BERT [34] and SimCSE [8], established the effectiveness of semantic embeddings for semantic tasks. More recently, the focus has shifted towards leveraging the sophisticated contextual understanding of LLMs to generate high-quality, context-aware embeddings [3, 21, 24]. These models have demonstrated state-of-the-art performance in various downstream applications [29, 38]. Our work does not propose a new representation model. Instead, we focus on the systems challenge of efficient workflow orchestration. ScaleDoc is designed to be agnostic to the specific technique, treating the semantic representation model as a pluggable component. This allows our system to seamlessly integrate and benefit from any effective LLM representing method during its offline processing phase.

Contrastive Learning Contrastive learning [5] is originally proposed as a self-supervised representation learning technique. By learning highly discriminative and robust semantic representations, contrastive learning-based methods prevail in Information Retrieval [17] and Multi-Modal tasks [22, 32]. With the contrastive learning paradigm, ScaleDoc effectively promotes the mining for latent relationships inside raw embeddings from the LLM encoders, enabling an adaptability for ad-hoc query semantics.

8 CONCLUSION

In this paper, we introduced ScaleDoc, a novel system designed to efficiently scale LLM-based semantic predicates over large document collections. It decouples the execution into an offline representation phase and a highly optimized online filtering phase. The system's effectiveness stems from two key innovations: (1) a query-aware proxy model to produce reliable predicating scores, and (2) an ad-hoc cascade workflow that dynamically determine the data filtering under specified accuracy targets. Experiments on diverse datasets confirm our design, showing ScaleDoc reduces LLM calls by up to 85% and accelerates end-to-end performance by over 2×. Our work highlights the potential for leveraging LLMs in large-scale data analysis systems with effective performance.

REFERENCES

[1] Amey Agrawal, Nitin Kedia, Ashish Panwar, Jayashree Mohan, Nipun Kwatra, Bhargav Gulavani, Alexey Tumanov, and Ramachandran Ramjee. 2024. Taming {Throughput-Latency} tradeoff in {LLM} inference with {Sarathi-Serve}. In *18th USENIX Symposium on Operating Systems Design and Implementation (OSDI 24)*. 117–134.

[2] Simran Arora, Brandon Yang, Sabri Eyuboglu, Avanika Narayan, Andrew Hojel, Immanuel Trummer, and Christopher Ré. 2023. Language Models Enable Simple Systems for Generating Structured Views of Heterogeneous Data Lakes. *Proceedings of the VLDB Endowment* 17, 2 (2023), 92–105.

[3] Parishad BehnamGhader, Vaibhav Adlakha, Marius Mosbach, Dzmitry Bahdanau, Nicolas Chapados, and Siva Reddy. 2024. LLM2Vec: Large Language Models Are Secretly Powerful Text Encoders. In *First Conference on Language Modeling*. https://openreview.net/forum?id=IW1PR7vEBf

[4] Lingjiao Chen, Matei Zaharia, and James Zou. 2023. FrugalGPT: How to Use Large Language Models While Reducing Cost and Improving Performance. arXiv:2305.05176 [cs.LG] https://arxiv.org/abs/2305.05176

[5] Ting Chen, Simon Kornblith, Mohammad Norouzi, and Geoffrey Hinton. 2020. A simple framework for contrastive learning of visual representations. In *International conference on machine learning*. PmLR, 1597–1607.

[6] Tri Dao, Dan Fu, Stefano Ermon, Atri Rudra, and Christopher Ré. 2022. Flashattention: Fast and memory-efficient exact attention with io-awareness. *Advances in neural information processing systems* 35 (2022), 16344–16359.

[7] Franck Dernoncourt and Ji Young Lee. 2017. PubMed 200k RCT: a Dataset for Sequential Sentence Classification in Medical Abstracts. In *Proceedings of the Eighth International Joint Conference on Natural Language Processing (Volume 2: Short Papers)*, Greg Kondrak and Taro Watanabe (Eds.). Asian Federation of Natural Language Processing, Taipei, Taiwan, 308–313. https://aclanthology.org/I17-2052/

[8] Tianyu Gao, Xingcheng Yao, and Danqi Chen. 2021. SimCSE: Simple Contrastive Learning of Sentence Embeddings. In *Proceedings of the 2021 Conference on Empirical Methods in Natural Language Processing*, Marie-Francine Moens, Xuanjing Huang, Lucia Specia, and Scott Wen-tau Yih (Eds.). Association for Computational Linguistics, Online and Punta Cana, Dominican Republic, 6894–6910. https://doi.org/10.18653/v1/2021.emnlp-main.552

[9] Aaron Grattafiori, Abhimanyu Dubey, Abhinav Jauhri, Abhinav Pandey, Abhishek Kadian, Ahmad Al-Dahle, Aiesha Letman, Akhil Mathur, Alan Schelten, Alex Vaughan, Amy Yang, Angela Fan, Anirudh Goyal, Anthony Hartshorn, Aobo Yang, Archi Mitra, Archie Sravankumar, Artem Korenev, Arthur Hinsvark, Arun Rao, Aston Zhang, Aurelien Rodriguez, Austen Gregerson, Ava Spataru, Baptiste Roziere, Bethany Biron, Binh Tang, Bobbie Chern, Charlotte Caucheteux, Chaya Nayak, Chloe Bi, Chris Marra, Chris McConnell, Christian Keller, Christophe Touret, Chunyang Wu, Corinne Wong, Cristian Canton Ferrer, Cyrus Nikolaidis, Damien Allonsius, Daniel Song, Danielle Pintz, Danny Livshits, Danny Wyatt, David Esiobu, Dhruv Choudhary, Dhruv Mahajan, Diego Garcia-Olano, Diego Perino, Dieuwke Hupkes, Egor Lakomkin, Ehab AlBadawy, Elina Lobanova, Emily Dinan, Eric Michael Smith, Filip Radenovic, Francisco Guzmán, Frank Zhang, Gabriel Synnaeve, Gabrielle Lee, Georgia Lewis Anderson, Govind Thattai, Graeme Nail, Gregoire Mialon, Guan Pang, Guillem Cucurell, Hailey Nguyen, Hannah Korevaar, Hu Xu, Hugo Touvron, Iliyan Zarov, Imanol Arrieta Ibarra, Isabel Kloumann, Ishan Misra, Ivan Evtimov, Jack Zhang, Jade Copet, Jaewon Lee, Jan Geffert, Jana Vranes, Jason Park, Jay Mahadeokar, Jeet Shah, Jelmer van der Linde, Jennifer Billock, Jenny Hong, Jenya Lee, Jeremy Fu, Jianfeng Chi, Jianyu Huang, Jiawen Liu, Jie Wang, Jiecao Yu, Joanna Bitton, Joe Spisak, Jongsoo Park, Joseph Rocca, Joshua Johnstun, Joshua Saxe, Junteng Jia, Kalyan Vasuden Alwala, Karthik Prasad, Kartikeya Upasani, Kate Plawiak, Ke Li, Kenneth Heafield, Kevin Stone, Khalid El-Arini, Krithika Iyer, Kshitiz Malik, Kuenley Chiu, Kunal Bhalla, Kushal Lakhotia, Lauren Rantala-Yeary, Laurens van der Maaten, Lawrence Chen, Liang Tan, Liz Jenkins, Louis Martin, Lovish Madaan, Lubo Malo, Lukas Blecher, Lukas Landzaat, Luke de Oliveira, Madeline Muzzi, Mahesh Pasupuleti, Mannat Singh, Manohar Paluri, Marcin Kardas, Maria Tsimpoukelli, Mathew Oldham, Mathieu Rita, Maya Pavlova, Melanie Kambadur, Mike Lewis, Min Si, Mitesh Kumar Singh, Mona Hassan, Naman Goyal, Narjes Torabi, Nikolay Bashlykov, Nikolay Bogoychev, Niladri Chatterji, Ning Zhang, Olivier Duchenne, Onur Çelebi, Patrick Alrassy, Pengchuan Zhang, Pengwei Li, Petar Vasic, Peter Weng, Prajjwal Bhargava, Pratik Dubal, Praveen Krishnan, Punit Singh Koura, Puxin Xu, Qing He, Qingxiao Dong, Ragavan Srinivasan, Raj Ganapathy, Ramon Calderer, Ricardo Silveira Cabral, Robert Stojnic, Roberta Raileanu, Rohan Maheswari, Rohit Girdhar, Rohit Patel, Romain Sauvestre, Ronnie Polidoro, Roshan Sumbaly, Ross Taylor, Ruan Silva, Rui Hou, Rui Wang, Saghar Hosseini, Sahana Chennabasappa, Sanjay Singh, Sean Bell, Seohyun Sonia Kim, Sergey Edunov, Shaoliang Nie, Sharan Narang, Sharath Raparthy, Sheng Shen, Shengye Wan, Shruti Bhosale, Shun Zhang, Simon Vandenhende, Soumya Batra, Spencer Whitman, Sten Sootla, Stephane Collot, Suchin Gururangan, Sydney Borodinsky, Tamar Herman, Tara Fowler, Tarek Sheasha, Thomas Georgiou, Thomas Scialom, Tobias Speckbacher, Todor Mihaylov, Tong Xiao, Ujjwal Karn, Vedanuj Goswami, Vibhor Gupta, Vignesh Ramanathan, Viktor Kerkez, Vincent Gonguet, Virginie Do, Vish Vogeti, Vítor Albiero, Vladan Petrovic, Weiwei Chu, Wenhan Xiong, Wenyin Fu, Whitney Meers, Xavier Martinet, Xiaodong Wang, Xiaofang Wang, Xiaoqing Ellen Tan, Xide Xia, Xinfeng Xie, Xuchao Jia, Xuewei Wang, Yaelle Goldschlag, Yashesh Gaur, Yasmine Babaei, Yi Wen, Yiwen Song, Yuchen Zhang, Yue Li, Yuning Mao, Zacharie Delpierre Coudert, Zheng Yan, Zhengxing Chen, Zoe Papakipos, Aaditya Singh, Aayushi Srivastava, Abha Jain, Adam Kelsey, Adam Shajnfeld, Adithya Gangidi, Adolfo Victoria, Ahuva Goldstand, Ajay Menon, Ajay Sharma, Alex Boesenberg, Alexei Baevski, Allie Feinstein, Amanda Kallet, Amit Sangani, Amos Teo, Anam Yunus, Andrei Lupu, Andres Alvarado, Andrew Caples, Andrew Gu, Andrew Ho, Andrew Poulton, Andrew Ryan, Ankit Ramchandani, Annie Dong, Annie Franco, Anuj Goyal, Aparajita Saraf, Arkabandhu Chowdhury, Ashley Gabriel, Ashwin Bharambe, Assaf Eisenman, Azadeh Yazdan, Beau James, Ben Maurer, Benjamin Leonhardi, Bernie Huang, Beth Loyd, Beto De Paola, Bhargavi Paranjape, Bing Liu, Bo Wu, Boyu Ni, Braden Hancock, Bram Wasti, Brandon Spence, Brani Stojkovic, Brian Gamido, Britt Montalvo, Carl Parker, Carly Burton, Catalina Mejia, Ce Liu, Changhan Wang, Changkyu Kim, Chao Zhou, Chester Hu, Ching-Hsiang Chu, Chris Cai, Chris Tindal, Christoph Feichtenhofer, Cynthia Gao, Damon Civin, Dana Beaty, Daniel Kreymer, Daniel Li, David Adkins, David Xu, Davide Testuggine, Delia David, Devi Parikh, Diana Liskovich, Didem Foss, Dingkang Wang, Duc Le, Dustin Holland, Edward Dowling, Eissa Jamil, Elaine Montgomery, Eleonora Presani, Emily Hahn, Emily Wood, Eric-Tuan Le, Erik Brinkman, Esteban Arcaute, Evan Dunbar, Evan Smothers, Fei Sun, Felix Kreuk, Feng Tian, Filippos Kokkinos, Firat Ozgenel, Francesco Caggioni, Frank Kanayet, Frank Seide, Gabriela Medina Florez, Gabriella Schwarz, Gada Badeer, Georgia Swee, Gil Halpern, Grant Herman, Grigory Sizov, Guangyi, Zhang, Guna Lakshminarayanan, Hakan Inan, Hamid Shojanazeri, Han Zou, Hannah Wang, Hanwen Zha, Haroun Habeeb, Harrison Rudolph, Helen Suk, Henry Aspegren, Hunter Goldman, Hongyuan Zhan, Ibrahim Damlaj, Igor Molybog, Igor Tufanov, Ilias Leontiadis, Irina-Elena Veliche, Itai Gat, Jake Weissman, James Geboski, James Kohli, Janice Lam, Japhet Asher, Jean-Baptiste Gaya, Jeff Marcus, Jeff Tang, Jennifer Chan, Jenny Zhen, Jeremy Reizenstein, Jeremy Teboul, Jessica Zhong, Jian Jin, Jingyi Yang, Joe Cummings, Jon Carvill, Jon Shepard, Jonathan McPhie, Jonathan Torres, Josh Ginsburg, Junjie Wang, Kai Wu, Kam Hou U, Karan Saxena, Kartikay Khandelwal, Katayoun Zand, Kathy Matosich, Kaushik Veeraraghavan, Kelly Michelena, Keqian Li, Kiran Jagadeesh, Kun Huang, Kunal Chawla, Kyle Huang, Lailin Chen, Lakshya Garg, Lavender A, Leandro Silva, Lee Bell, Lei Zhang, Liangpeng Guo, Licheng Yu, Liron Moshkovich, Luca Wehrstedt, Madian Khabsa, Manav Avalani, Manish Bhatt, Martynas Mankus, Matan Hasson, Matthew Lennie, Matthias Reso, Maxim Groshev, Maxim Naumov, Maya Lathi, Meghan Keneally, Miao Liu, Michael L. Seltzer, Michal Valko, Michelle Restrepo, Mihir Patel, Mik Vyatskov, Mikayel Samvelyan, Mike Clark, Mike Macey, Mike Wang, Miquel Jubert Hermoso, Mo Metanat, Mohammad Rastegari, Munish Bansal, Nandhini Santhanam, Natascha Parks, Natasha White, Navyata Bawa, Nayan Singhal, Nick Egebo, Nicolas Usunier, Nikhil Mehta, Nikolay Pavlovich Laptev, Ning Dong, Norman Cheng, Oleg Chernoguz, Olivia Hart, Omkar Salpekar, Ozlem Kalinli, Parkin Kent, Parth Parekh, Paul Saab, Pavan Balaji, Pedro Rittner, Philip Bontrager, Pierre Roux, Piotr Dollar, Polina Zvyagina, Prashant Ratanchandani, Pritish Yuvraj, Qian Liang, Rachad Alao, Rachel Rodriguez, Rafi Ayub, Raghotham Murthy, Raghu Nayani, Rahul Mitra, Rangaprabhu Parthasarathy, Raymond Li, Rebekkah Hogan, Robin Battey, Rocky Wang, Russ Howes, Ruty Rinott, Sachin Mehta, Sachin Siby, Sai Jayesh Bondu, Samyak Datta, Sara Chugh, Sara Hunt, Sargun Dhillon, Sasha Sidorov, Satadru Pan, Saurabh Mahajan, Saurabh Verma, Seiji Yamamoto, Sharadh Ramaswamy, Shaun Lindsay, Shaun Lindsay, Sheng Feng, Shenghao Lin, Shengxin Cindy Zha, Shishir Patil, Shiva Shankar, Shuqiang Zhang, Shuqiang Zhang, Sinong Wang, Sneha Agarwal, Soji Sajuyigbe, Soumith Chintala, Stephanie Max, Stephen Chen, Steve Kehoe, Steve Satterfield, Sudarshan Govindaprasad, Sumit Gupta, Summer Deng, Sungmin Cho, Sunny Virk, Suraj Subramanian, Sy Choudhury, Sydney Goldman, Tal Remez, Tamar Glaser, Tamara Best, Thilo Koehler, Thomas Robinson, Tianhe Li, Tianjun Zhang, Tim Matthews, Timothy Chou, Tzook Shaked, Varun Vontimitta, Victoria Ajayi, Victoria Montanez, Vijai Mohan, Vinay Satish Kumar, Vishal Mangla, Vlad Ionescu, Vlad Poenaru, Vlad Tiberiu Mihailescu, Vladimir Ivanov, Wei Li, Wenchen Wang, Wenwen Jiang, Wes Bouaziz, Will Constable, Xiaocheng Tang, Xiaojian Wu, Xiaolan Wang, Xilun Wu, Xinbo Gao, Yaniv Kleinman, Yanjun Chen, Ye Hu, Ye Jia, Ye Qi, Yenda Li, Yilin Zhang, Ying Zhang, Yossi Adi, Youngjin Nam, Yu, Wang, Yu Zhao, Yuchen Hao, Yundi Qian, Yunlu Li, Yuzi He, Zach Rait, Zachary DeVito, Zef Rosnbrick, Zhaoduo Wen, Zhenyu Yang, Zhiwei Zhao, and Zhiyu Ma. 2024. The Llama 3 Herd of Models. arXiv:2407.21783 [cs.AI] https://arxiv.org/abs/2407.21783

[10] Kaiming He, Haoqi Fan, Yuxin Wu, Saining Xie, and Ross Girshick. 2020. Momentum contrast for unsupervised visual representation learning. In *Proceedings of the IEEE/CVF conference on computer vision and pattern recognition*. 9729–9738.

[11] Chuxuan Hu, Austin Peters, and Daniel Kang. 2025. LEAP: LLM-powered End-to-end Automatic Library for Processing Social Science Queries on Unstructured Data. *arXiv preprint arXiv:2501.03892* (2025).

[12] Luyang Huang, Shuyang Cao, Nikolaus Parulian, Heng Ji, and Lu Wang. 2021. Efficient Attentions for Long Document Summarization. In *Proceedings of the 2021 Conference of the North American Chapter of the Association for Computational Linguistics: Human Language Technologies*. Association for Computational

Linguistics, Online, 1419–1436. https://doi.org/10.18653/v1/2021.naacl-main.112

[13] Yulong Hui, Yao Lu, and Huanchen Zhang. [n.d.]. UDA: A Benchmark Suite for Retrieval Augmented Generation in Real-World Document Analysis. In *The Thirty-eight Conference on Neural Information Processing Systems Datasets and Benchmarks Track*.

[14] Albert Q. Jiang, Alexandre Sablayrolles, Arthur Mensch, Chris Bamford, Devendra Singh Chaplot, Diego de las Casas, Florian Bressand, Gianna Lengyel, Guillaume Lample, Lucile Saulnier, Lélio Renard Lavaud, Marie-Anne Lachaux, Pierre Stock, Teven Le Scao, Thibaut Lavril, Thomas Wang, Timothée Lacroix, and William El Sayed. 2023. Mistral 7B. arXiv:2310.06825 [cs.CL] https://arxiv.org/abs/2310.06825

[15] Daniel Kang, John Emmons, Firas Abuzaid, Peter Bailis, and Matei Zaharia. 2017. NoScope: Optimizing Neural Network Queries over Video at Scale. *Proceedings of the VLDB Endowment* 10, 11 (2017).

[16] Daniel Kang, Edward Gan, Peter Bailis, Tatsunori Hashimoto, and Matei Zaharia. 2020. Approximate selection with guarantees using proxies. *arXiv preprint arXiv:2004.00827* (2020).

[17] Vladimir Karpukhin, Barlas Oguz, Sewon Min, Ledell Wu, Sergey Edunov, Danqi Chen, and Wen-tau Yih. [n.d.]. Dense Passage Retrieval for Open-Domain Question Answering.

[18] Moe Kayali, Anton Lykov, Ilias Fountalis, Nikolaos Vasiloglou, Dan Olteanu, and Dan Suciu. 2024. Chorus: Foundation Models for Unified Data Discovery and Exploration. *Proceedings of the VLDB Endowment* 17, 8 (2024), 2104–2114.

[19] Prannay Khosla, Piotr Teterwak, Chen Wang, Aaron Sarna, Yonglong Tian, Phillip Isola, Aaron Maschinot, Ce Liu, and Dilip Krishnan. 2020. Supervised contrastive learning. *Advances in neural information processing systems* 33 (2020), 18661–18673.

[20] Woosuk Kwon, Zhuohan Li, Siyuan Zhuang, Ying Sheng, Lianmin Zheng, Cody Hao Yu, Joseph Gonzalez, Hao Zhang, and Ion Stoica. 2023. Efficient memory management for large language model serving with pagedattention. In *Proceedings of the 29th Symposium on Operating Systems Principles*. 611–626.

[21] Chankyu Lee, Rajarshi Roy, Mengyao Xu, Jonathan Raiman, Mohammad Shoeybi, Bryan Catanzaro, and Wei Ping. 2024. Nv-embed: Improved techniques for training llms as generalist embedding models. *arXiv preprint arXiv:2405.17428* (2024).

[22] Junnan Li, Dongxu Li, Silvio Savarese, and Steven Hoi. 2023. Blip-2: Bootstrapping language-image pre-training with frozen image encoders and large language models. In *International conference on machine learning*. PMLR, 19730–19742.

[23] Zhenwen Li and Tao Xie. 2024. Using LLM to select the right SQL Query from candidates. *arXiv preprint arXiv:2401.02115* (2024).

[24] Zehan Li, Xin Zhang, Yanzhao Zhang, Dingkun Long, Pengjun Xie, and Meishan Zhang. 2023. Towards general text embeddings with multi-stage contrastive learning. *arXiv preprint arXiv:2308.03281* (2023).

[25] Chunwei Liu, Matthew Russo, Michael Cafarella, Lei Cao, Peter Baille Chen, Zui Chen, Michael Franklin, Tim Kraska, Samuel Madden, and Gerardo Vitagliano. 2024. A declarative system for optimizing ai workloads. *arXiv preprint arXiv:2405.14696* (2024).

[26] Shicheng Liu, Jialiang Xu, Wesley Tjangnaka, Sina Semnani, Chen Yu, and Monica Lam. 2024. SUQL: Conversational Search over Structured and Unstructured Data with Large Language Models. In *Findings of the Association for Computational Linguistics: NAACL 2024*, Kevin Duh, Helena Gomez, and Steven Bethard (Eds.). Association for Computational Linguistics, Mexico City, Mexico, 4535–4555. https://doi.org/10.18653/v1/2024.findings-naacl.283

[27] Yao Lu, Aakanksha Chowdhery, Srikanth Kandula, and Surajit Chaudhuri. 2018. Accelerating machine learning inference with probabilistic predicates. In *Proceedings of the 2018 International Conference on Management of Data*. 1493–1508.

[28] Kyle Luoma and Arun Kumar. 2025. SNAILS: Schema Naming Assessments for Improved LLM-Based SQL Inference. *Proceedings of the ACM on Management of Data* 3, 1 (2025), 1–26.

[29] Jianmo Ni, Chen Qu, Jing Lu, Zhuyun Dai, Gustavo Hernandez Abrego, Ji Ma, Vincent Zhao, Yi Luan, Keith Hall, Ming-Wei Chang, et al. 2022. Large Dual Encoders Are Generalizable Retrievers. In *Proceedings of the 2022 Conference on Empirical Methods in Natural Language Processing*. 9844–9855.

[30] OpenAI, Aaron Hurst, Adam Lerer, Adam P. Goucher, Adam Perelman, Aditya Ramesh, Aidan Clark, AJ Ostrow, Akila Welihinda, Alan Hayes, Alec Radford, Aleksander Mądry, Alex Baker-Whitcomb, Alex Beutel, Alex Borzunov, Alex Carney, Alex Chow, Alex Kirillov, Alex Nichol, Alex Paino, Alex Renzin, Alex Tachard Passos, Alexander Kirillov, Alexi Christakis, Alexis Conneau, Ali Kamali, Allan Jabri, Allison Moyer, Allison Tam, Amadou Crookes, Amin Tootoochian, Amin Tootoonchian, Ananya Kumar, Andrea Vallone, Andrej Karpathy, Andrew Braunstein, Andrew Cann, Andrew Codispoti, Andrew Galu, Andrew Kondrich, Andrew Tulloch, Andrey Mishchenko, Angela Baek, Angela Jiang, Antoine Pelisse, Antonia Woodford, Anuj Gosalia, Arka Dhar, Ashley Pantuliano, Avi Nayak, Avital Oliver, Barret Zoph, Behrooz Ghorbani, Ben Leimberger, Ben Rossen, Ben Sokolowsky, Ben Wang, Benjamin Zweig, Beth Hoover, Blake Samic, Bob McGrew, Bobby Spero, Bogo Giertler, Bowen Cheng, Brad Lightcap, Brandon Walkin, Brendan Quinn, Brian Guarraci, Brian Hsu, Bright Kellogg, Brydon Eastman, Camillo Lugaresi, Carroll Wainwright, Cary Bassin, Cary Hudson, Casey Chu, Chad Nelson, Chak Li, Chan Jun Shern, Channing Conger, Charlotte Barette, Chelsea Voss, Chen Ding, Cheng Lu, Chong Zhang, Chris Beaumont, Chris Hallacy, Chris Koch, Christian Gibson, Christina Kim, Christine Choi, Christine McLeavey, Christopher Hesse, Claudia Fischer, Clemens Winter, Coley Czarnecki, Colin Jarvis, Colin Wei, Constantin Koumouzelis, Dane Sherburn, Daniel Kappler, Daniel Levin, Daniel Levy, David Carr, David Farhi, David Mely, David Robinson, David Sasaki, Denny Jin, Dev Valladares, Dimitris Tsipras, Doug Li, Duc Phong Nguyen, Duncan Findlay, Edede Oiwoh, Edmund Wong, Ehsan Asdar, Elizabeth Proehl, Elizabeth Yang, Eric Antonow, Eric Kramer, Eric Peterson, Eric Sigler, Eric Wallace, Eugene Brevdo, Evan Mays, Farzad Khorasani, Felipe Petroski Such, Filippo Raso, Francis Zhang, Fred von Lohmann, Freddie Sulit, Gabriel Goh, Gene Oden, Geoff Salmon, Giulio Starace, Greg Brockman, Hadi Salman, Haiming Bao, Haitang Hu, Hannah Wong, Haoyu Wang, Heather Schmidt, Heather Whitney, Heewoo Jun, Hendrik Kirchner, Henrique Ponde de Oliveira Pinto, Hongyu Ren, Huiwen Chang, Hyung Won Chung, Ian Kivlichan, Ian O'Connell, Ian O'Connell, Ian Osband, Ian Silber, Ian Sohl, Ibrahim Okuyucu, Ikai Lan, Ilya Kostrikov, Ilya Sutskever, Ingmar Kanitscheider, Ishaan Gulrajani, Jacob Coxon, Jacob Menick, Jakub Pachocki, James Aung, James Betker, James Crooks, James Lennon, Jamie Kiros, Jan Leike, Jane Park, Jason Kwon, Jason Phang, Jason Teplitz, Jason Wei, Jason Wolfe, Jay Chen, Jeff Harris, Jenia Varavva, Jessica Gan Lee, Jessica Shieh, Ji Lin, Jiahui Yu, Jiayi Weng, Jie Tang, Jieqi Yu, Joanne Jang, Joaquin Quinonero Candela, Joe Beutler, Joe Landers, Joel Parish, Johannes Heidecke, John Schulman, Jonathan Lachman, Jonathan McKay, Jonathan Uesato, Jonathan Ward, Jong Wook Kim, Joost Huizinga, Jordan Sitkin, Jos Kraaijeveld, Josh Gross, Josh Kaplan, Josh Snyder, Joshua Achiam, Joy Jiao, Joyce Lee, Juntang Zhuang, Justyn Harriman, Kai Fricke, Kai Hayashi, Karan Singhal, Katy Shi, Kavin Karthik, Kayla Wood, Kendra Rimbach, Kenny Hsu, Kenny Nguyen, Keren Gu-Lemberg, Kevin Button, Kevin Liu, Kiel Howe, Krithika Muthukumar, Kyle Luther, Lama Ahmad, Larry Kai, Lauren Itow, Lauren Workman, Leher Pathak, Leo Chen, Li Jing, Lia Guy, Liam Fedus, Liang Zhou, Lien Mamitsuka, Lilian Weng, Lindsay McCallum, Lindsey Held, Long Ouyang, Louis Feuvrier, Lu Zhang, Lukas Kondraciuk, Lukasz Kaiser, Luke Hewitt, Luke Metz, Lyric Doshi, Mada Aflak, Maddie Simens, Madelaine Boyd, Madeleine Thompson, Marat Dukhan, Mark Chen, Mark Gray, Mark Hudnall, Marvin Zhang, Marwan Aljubeh, Mateusz Litwin, Matthew Zeng, Max Johnson, Maya Shetty, Mayank Gupta, Meghan Shah, Mehmet Yatbaz, Meng Jia Yang, Mengchao Zhong, Mia Glaese, Mianna Chen, Michael Janner, Michael Lampe, Michael Petrov, Michael Wu, Michele Wang, Michelle Fradin, Michelle Pokrass, Miguel Castro, Miguel Oom Temudo de Castro, Mikhail Pavlov, Miles Brundage, Miles Wang, Minal Khan, Mira Murati, Mo Bavarian, Molly Lin, Murat Yesildal, Nacho Soto, Natalia Gimelshein, Natalie Cone, Natalie Staudacher, Natalie Summers, Natan LaFontaine, Neil Chowdhury, Nick Ryder, Nick Stathas, Nick Turley, Nik Tezak, Niko Felix, Nithanth Kudige, Nitish Keskar, Noah Deutsch, Noel Bundick, Nora Puckett, Ofir Nachum, Ola Okelola, Oleg Boiko, Oleg Murk, Oliver Jaffe, Olivia Watkins, Olivier Godement, Owen Campbell-Moore, Patrick Chao, Paul McMillan, Pavel Belov, Peng Su, Peter Bak, Peter Bakkum, Peter Deng, Peter Dolan, Peter Hoeschele, Peter Welinder, Phil Tillet, Philip Pronin, Philippe Tillet, Prafulla Dhariwal, Qiming Yuan, Rachel Dias, Rachel Lim, Rahul Arora, Rajan Troll, Randall Lin, Rapha Gontijo Lopes, Raul Puri, Reah Miyara, Reimar Leike, Renaud Gaubert, Reza Zamani, Ricky Wang, Rob Donnelly, Rob Honsby, Rocky Smith, Rohan Sahai, Rohit Ramchandani, Romain Huet, Rory Carmichael, Rowan Zellers, Roy Chen, Ruby Chen, Ruslan Nigmatullin, Ryan Cheu, Saachi Jain, Sam Altman, Sam Schoenholz, Sam Toizer, Samuel Miserendino, Sandhini Agarwal, Sara Culver, Scott Ethersmith, Scott Gray, Sean Grove, Sean Metzger, Shamez Hermani, Shantanu Jain, Shengjia Zhao, Sherwin Wu, Shino Jomoto, Shirong Wu, Shuaiqi, Xia, Sonia Phene, Spencer Papay, Srinivas Narayanan, Steve Coffey, Steve Lee, Stewart Hall, Suchir Balaji, Tal Broda, Tal Stramer, Tao Xu, Tarun Gogineni, Taya Christianson, Ted Sanders, Tejal Patwardhan, Thomas Cunninghman, Thomas Degry, Thomas Dimson, Thomas Raoux, Thomas Shadwell, Tianhao Zheng, Todd Underwood, Todor Markov, Toki Sherbakov, Tom Rubin, Tom Stasi, Tomer Kaftan, Tristan Heywood, Troy Peterson, Tyce Walters, Tyna Eloundou, Valerie Qi, Veit Moeller, Vinnie Monaco, Vishal Kuo, Vlad Fomenko, Wayne Chang, Weiyi Zheng, Wenda Zhou, Wesam Manassra, Will Sheu, Wojciech Zaremba, Yash Patil, Yilei Qian, Yongjik Kim, Youlong Cheng, Yu Zhang, Yuchen He, Yuchen Zhang, Yujia Jin, Yunxing Dai, and Yury Malkov. 2024. GPT-4o System Card. arXiv:2410.21276 [cs.CL] https://arxiv.org/abs/2410.21276

[31] Liana Patel, Siddharth Jha, Carlos Guestrin, and Matei Zaharia. 2024. Lotus: Enabling semantic queries with llms over tables of unstructured and structured data. *arXiv preprint arXiv:2407.11418* (2024).

[32] Alec Radford, Jong Wook Kim, Chris Hallacy, Aditya Ramesh, Gabriel Goh, Sandhini Agarwal, Girish Sastry, Amanda Askell, Pamela Mishkin, Jack Clark, et al. 2021. Learning transferable visual models from natural language supervision. In *International conference on machine learning*. PmLR, 8748–8763.

[33] Abhinav Ramesh Kashyap, Thanh-Tung Nguyen, Viktor Schlegel, Stefan Winkler, See-Kiong Ng, and Soujanya Poria. 2024. A Comprehensive Survey of Sentence Representations: From the BERT Epoch to the CHATGPT Era and Beyond. In *Proceedings of the 18th Conference of the European Chapter of the Association for Computational Linguistics (Volume 1: Long Papers)*, Yvette Graham and Matthew Purver (Eds.). Association for Computational Linguistics, St. Julian's, Malta,

1738–1751. https://aclanthology.org/2024.eacl-long.104/

[34] Nils Reimers and Iryna Gurevych. 2019. Sentence-BERT: Sentence Embeddings using Siamese BERT-Networks. In *Proceedings of the 2019 Conference on Empirical Methods in Natural Language Processing and the 9th International Joint Conference on Natural Language Processing (EMNLP-IJCNLP)*. 3982–3992.

[35] Ricardo Salazar-Díaz, Boris Glavic, and Tilmann Rabl. 2024. Inferdb: In-database machine learning inference using indexes. *Proceedings of the VLDB Endowment* 17, 8 (2024), 1830–1842.

[36] Shreya Shankar, Tristan Chambers, Tarak Shah, Aditya G Parameswaran, and Eugene Wu. 2024. DocETL: Agentic Query Rewriting and Evaluation for Complex Document Processing. *arXiv preprint arXiv:2410.12189* (2024).

[37] Eva Sharma, Chen Li, and Lu Wang. 2019. BIGPATENT: A Large-Scale Dataset for Abstractive and Coherent Summarization. In *Proceedings of the 57th Annual Meeting of the Association for Computational Linguistics*, Anna Korhonen, David Traum, and Lluís Màrquez (Eds.). Association for Computational Linguistics, Florence, Italy, 2204–2213. https://doi.org/10.18653/v1/P19-1212

[38] Hongjin Su, Weijia Shi, Jungo Kasai, Yizhong Wang, Yushi Hu, Mari Ostendorf, Wen-tau Yih, Noah A Smith, Luke Zettlemoyer, and Tao Yu. 2023. One Embedder, Any Task: Instruction-Finetuned Text Embeddings. In *Annual Meeting of the Association for Computational Linguistics-ACL 2023 (09/07/2023-14/07/2023,,, Toronto, Canada)*.

[39] Zhihui Yang, Zuozhi Wang, Yicong Huang, Yao Lu, Chen Li, and X Sean Wang. 2022. Optimizing machine learning inference queries with correlative proxy models. *Proceedings of the VLDB Endowment* 15, 10 (2022), 2032–2044.

[40] Enhao Zhang, Nicole Sullivan, Brandon Haynes, Ranjay Krishna, and Magdalena Balazinska. 2025. Self-Enhancing Video Data Management System for Compositional Events with Large Language Models. *Proc. ACM Manag. Data* 3, 3, Article 215 (June 2025), 29 pages. https://doi.org/10.1145/3725352

[41] Shuo Zhang, Zezhou Huang, and Eugene Wu. 2024. Data cleaning using large language models. *arXiv preprint arXiv:2410.15547* (2024).

[42] Yinmin Zhong, Shengyu Liu, Junda Chen, Jianbo Hu, Yibo Zhu, Xuanzhe Liu, Xin Jin, and Hao Zhang. 2024. DistServe: disaggregating prefill and decoding for goodput-optimized large language model serving. In *Proceedings of the 18th USENIX Conference on Operating Systems Design and Implementation* (Santa Clara, CA, USA) *(OSDI'24)*. USENIX Association, USA, Article 11, 18 pages.